Site occupancy in the Re-W sigma phase

C. Berne,[1] M. Sluiter,[2] Y. Kawazoe,[2] T. Hansen,[3] and A. Pasturel[4]
[1]*Commissariat à l'Energie Atomique, Direction de la Recherche Technologique, Département des Techniques des Energies Nouvelles, 17 Rue des Martyrs, 38054 Grenoble-Cedex 09, France*
[2]*Institute for Materials Research, Tohoku University, Sendai 980-8577, Japan*
[3]*Institut Laue Langevin, BP 156, 38042 Grenoble-Cedex 09, France*
[4]*Laboratoire de Physique et Modélisation des Milieux Condensés, Maison des Magistères, BP 166 CNRS, 38042 Grenoble-Cedex 09, France*
(Received 23 April 2001; published 19 September 2001)

The site occupancy in the Re-W sigma phase is studied using neutron-diffraction experiments and using a first-principles statistical thermodynamics approach. We show that the five inequivalent lattice sites of the sigma phase display a specific site-occupation sequence with increasing W composition which is explained by a theoretical analysis.

DOI: 10.1103/PhysRevB.64.144103 PACS number(s): 61.12.Ld, 61.66.Dk, 64.60.Cn, 71.20.Be

I. INTRODUCTION

Ordering processes are of primary importance in understanding crystal chemistry as well as relative phase stability and physical properties of substitutional alloys. During the last decade, a theoretical approach[1,2] combining electronic structure calculations and statistical studies has been used successfully to predict these effects. However, in most cases the alloys studied were based on simple underlying crystalline structures with just one or two atoms in the unit cell, such as fcc, bcc, or hcp. Conversely, few theoretical studies have been devoted to investigate the interplay between electronic properties and configurational order in substitutional alloys exhibiting complex crystallographic arrangement as in the case of the so-called Frank-Kasper (FK) phases.[3] The study of these complex structures is of fundamental interest because they display structural units that are believed to be present in nonperiodic systems. They are also very important for technological reasons because their presence is known to deteriorate mechanical properties of many commercial alloys. It is now well established that FK phases like *A*15, sigma, or chi satisfy the Goldschmidt-Hume Rothery's rule that suggests their formation to be electronically driven.[3]

For transition-metal-based alloys, a systematic treatment of the FK phases was formulated by Watson and Bennett.[4] Their empirical approach indicated that the average filling of the *d* band is important to predict which alloys form FK phases. Previous theoretical work based on tight-binding arguments[5,6] suggests that electronic effects and more particularly the *d*-band filling are crucial to explain the stability of the *A*15-based structure. To study ordering effects in *A*15-based alloys, Turchi and Finel[7] proposed to couple tight-binding calculations in the context of the generalized perturbation method (GPM) (Ref. 8) with a statistical thermodynamics method such as the cluster variation method (CVM) (Ref. 9) or the Monte Carlo method. Their main conclusion is that order-disorder phenomena in *A*15-based alloys are much more complex than in simple structure-based alloys.

The possibility of different order-disorder phenomena in complex structures motivated one of us (Sluiter) and co-workers[10] to study the Fe-Cr sigma phase. The Fe-Cr sigma phase was selected because much experimental work has been done on this material.[11,12] The main result is that the theoretical site occupation in the Fe-Cr sigma phase displays a peculiar behavior which is not in complete agreement with experiment and exhibits an occupancy reversal phenomenon. As a result, it seems to be crucial to test this theoretical approach on other systems to see if the occupancy reversal phenomenon is a common behavior of the sigma phase or if it is just a characteristic of the Fe-Cr system.

In this work we address this problem by combining neutron-diffraction analysis with first-principles-based calculations in studying the site occupancy in the Re-W sigma phase. The Re-W sigma phase was selected because it exists over a wide range of compositions, about 30–57 at. % W. In Sec. II, we present the details of our neutron measurements of the site occupation in the Re-W sigma phase. In Sec. III, we recall how first-principles calculations can be used to determine the site occupancy. Finally in Sec. IV, we summarize the use of both first-principles and neutron methods in describing the local order in the Re-W sigma phase.

II. EXPERIMENTAL DETAILS AND DATA ANALYSIS

The unit cell of the sigma phase contains 30 atoms that pertain to five crystallographically inequivalent sites *A*, *B*, *C*, *D*, and *E* with the occupation numbers 2, 4, 8, 8, and 8,

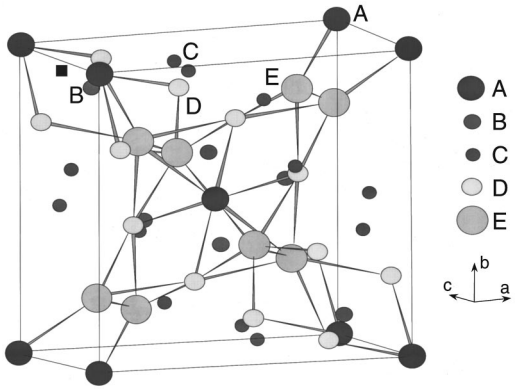

FIG. 1. Unit cell of the sigma phase.

TABLE I. Experimental occupancy of the inequivalent sites for the three compositions of the sigma ReW alloy.

Site	σ-ReW 34% W	σ-ReW 44% W	σ-ReW 54% W
A	5% W±3%	7% W±3%	16% W±3%
B	60% W±2%	72% W±2%	92% W±2%
C	46% W±2%	62% W±3%	75% W±1%
D	2% W±4%	8% W±3%	6% W±2%
E	47% W±2%	56% W±2%	70% W±1%

respectively[13] (see Fig. 1). Its space group is $P4_2/mnm$ and the corresponding Pearson symbol is $tP30$. Three types of coordination occur: the *A* and *D* sites are icosahedrally coordinated, the *B* site has 15 nearest neighbors, and the *C* and *E* sites are 14-fold coordinated.

Neutron diffraction was used to determine experimentally the atom distribution in the Re-W sigma phase. Re and W are neighbor elements in the Periodic Table and therefore exhibit almost no x-ray scattering contrast. Fortunately, Re and W have very different bound scattering lengths [bc(W) $=4.77$ fm, bc(Re)$=9.2$ fm] and thus there is good neutron-scattering contrast. In order to measure site occupancy in the sigma phase as a function of composition, three compositions were selected: 34% W, 44% W, and 54% W. These samples were prepared in the 50-m-high drop tube facility of the CEA-Grenoble, France.

Intensity data were collected on the high-resolution biaxial diffractometer D2B at the Institut Laue Langevin (ILL) facility in Grenoble, France. The incident wavelength used was 1.6 Å. The samples were powdered and placed in a vanadium cylindrical container (Debye Scherrer configuration). The diffraction data were analyzed by means of the Rietveld method for crystal structure refinement[14] using the computer program FULLPROF by Rodriguez Carjaval.[15] In this method the measured pattern is fitted to a model pattern that is calculated from sample parameters (space-group symmetry, lattice constants, atom parameters), and instruments parameters (wavelength, peak shape, peak width).

In the profile refinements parameters were chosen as follows. The background was interpolated between a set of manually determined points. The peak shape was described using a pseudo-Voigt function refined to be half Gaussian, half Lorentzian, indicating good crystallized samples. The Caglioti[16] coefficients modeling the full width at half maximum of Bragg peaks were refined close to the reference resolution function of the D2B diffractometer. The other parameters refined are the zero point, the cell parameters, the atomic positions of the atoms and the corresponding Debye-Waller factor, taken identical for all atoms. Finally the distribution of chemical species among the five sites is refined and thereby determined.

The results for the three different compositions are reported in Table I. We can see that Re is found to show a strong preference for *A* and *D* sites while W is strongly attracted to the highest coordinated *B* site. These results seem to be independent of the composition and will be discussed in relation with the theoretical results in Sec. IV.

TABLE II. Coordinates of the five inequivalent sites of the tetragonal sigma phase in units of *a* and *c*, respectively.

Site	Wyckoff position	Coordinates	
A	2(*a*)	0, 0, 0	1/2, 1/2, 1/2
B	4(*f*)	$x, x, 0$	$\overline{x}, \overline{x}, 0$
		$1/2+x, 1/2-x, 1/2$	$1/2-x, 1/2+x, 1/2$
		$x=0.398$	
C	8(*i*)	$x, y, 0$	$\overline{x}, \overline{y}, 0$
		$1/2+x, 1/2-y, 1/2$	$1/2-x, 1/2+y, 1/2$
		$y, x, 0$	$\overline{y}, \overline{x}, 0$
		$1/2+y, 1/2-x, 1/2$	$1/2-y, 1/2+x, 1/2$
		$x=0.463, y=0.131$	
D	8(*i*)	$x=0.739, y=0.066$	
E	8(*j*)	x, x, z	$\overline{x}, \overline{x}, z$
		$1/2+x, 1/2-x, 1/2+z$	$1/2-x, 1/2+x, 1/2+z$
		$x, x, \overline{z}$	$\overline{x}, \overline{x}, \overline{z}$
		$1/2+x, 1/2-x, 1/2-z$	$1/2-x, 1/2+x, 1/2-z$
		$x=0.183, z=0.25$	

III. FIRST-PRINCIPLES STUDY OF THE Re-W SIGMA PHASE

For a theoretical phase stability study of the sigma phase the Ising model can be used. The energetics associated with changing local atomic configurations is parameterized by a set of effective cluster interactions (ECI's) which can be formally defined in terms of linear combinations of configurationally averaged total energies of the system.[17] These ECI's can be calculated using any of a variety of first-principles techniques; following previous work,[10] we choose to use the Connolly-Williams method (CWM) (Ref. 18) to extract ECI's noted V_i, from the formation energies of different configurations. The five inequivalent sites of the sigma phase make $2^5=32$ possible distributions of Re and W atoms. These 32 configurations are not superstructures of the sigma phase because they all have the same space group. In addition, ten sigma superstructures were considered. The sigma superstructures make it possible to determine the pair interactions between sites of the same type (i.e., *B-B*-, *C-C*-, *D-D*-, and *E-E*-type pairs). In all, $32+10$ structures were used for the determination of the ECI's. In the CWM method, the effective interactions are determined by solving a linear system given by

$$E^{\alpha}_{\text{form}} = \sum_i \xi^{\alpha}_i V_i , \tag{1}$$

where the label α represents one of the 42 configurations and ξ^{α}_i refers to the correlation function pertaining to cluster *i*. A correlation function is given by the expectation value of the product of the occupation numbers for the sites in the cluster. The occupation number for the W (Re) atomic species were not selected as -1 (1) as is customary, but rather as 0 (1). This means that a correlation function takes a value that cor-

TABLE III. Optimized coordinates of the five inequivalent sites for pure Re and pure W.

Site	Position	Relaxed Re-σ coordinates	Relaxed W-σ coordinates
A	2(*a*)	0, 0, 0	0, 0, 0
B	4(*f*)	$x=0.405$	$x=0.400$
C	8(*i*)	$x=0.463$, $y=0.135$	$x=0.467$, $y=0.130$
D	8(*i*)	$x=0.738$, $y=0.066$	$x=0.742$, $y=0.060$
E	8(*j*)	$x=0.183$, $z=0.251$	$x=0.188$, $z=0.252$
Cell parameters		$a=9.558$ Å $c=4.970$ Å	$a=9.779$ Å $c=5.085$ Å

responds to the probability that the cluster has pure W occupancy.[19] A singular value decomposition algorithm[20] was used to extract the values for 29 effective interactions including the empty cluster. The other interactions are the 5 single-site terms, 18 pair terms, 4 triplet terms and 1 quadruplet term.

The formation energies E_{form} are obtained from the total energies by substracting the concentration weighted total energies of pure Re and W with the sigma structure. To compute total energies, we used the Vienna Ab Initio Simulation Package (VASP).[21] Ultrasoft pseudopotentials are used to approximate the electron-ion interactions with a plane-wave cutoff energy of 193.87 eV.[22] Bands near the Fermi surface are partially occupied using finite-temperature broadening as proposed by Methfessel and Paxton.[23] Integrations in reciprocal space use 18 *k* points in the irreducible Brillouin zone and a broadening parameter of 0.10 eV. The *a* and *c* parameters of the tetragonal unit cell and the cell internal coordinates were optimized for all configurations using a conjugate gradient method.[21] A previous study showed that results based on ultrasoft pseudopotentials are in good agreement with full potential linear muffin-tin orbital calculations.[24]

The interactions are then used to compute the site occupancy, entropy, and Gibbs free energy of the sigma phase as a function of temperature and composition within the tetrahedron approximation of the cluster variation method (CVM). The tetrahedron approximation gives 17 maximal clusters and 71 correlation functions.[10]

IV. DISCUSSION

A. Determination of the effective cluster interactions

In order to check the effects of the geometry optimization on the ECI's, two series of calculations were performed. As already mentioned, the geometry optimization of the sigma phase consists in determining the *a* and *c* parameters of the tetragonal unit cell as well as the internal atomic coordinates displayed in Table II. In a first set of calculations (unrelaxed), *a* and *c* parameters were optimized for pure Re and pure W and a linear interpolation scheme was used to obtain *a* and *c* for all other configurations. In this set of calculations, the atomic coordinates were held fixed as listed in Table II.[13] In the second set of calculations (relaxed), a full optimization

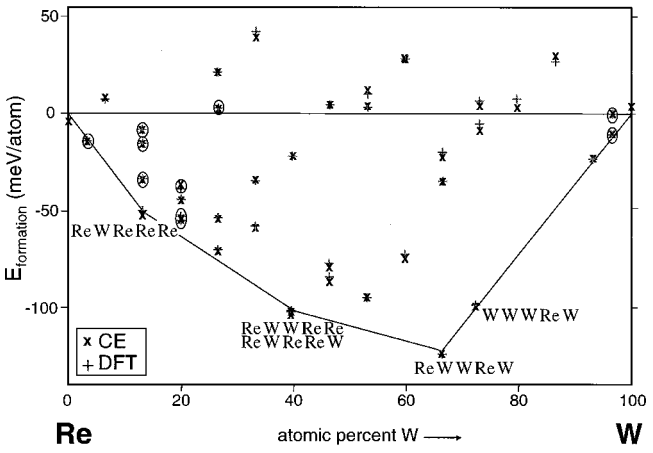

FIG. 2. Formation energy (in meV/atom) of nonrelaxed atomic configurations with the sigma structure: as computed with VASP (+); as computed from the effective interactions (×). Circles indicate the sigma superstructures. The most stable configurations have been connected with a solid line and the occupancy of the *A*, *B*, *C*, *D*, and *E* sites have been indicated.

including both unit-cell parameters and internal atomic coordinates was performed for each configuration. Table III gives the optimized internal atomic coordinates for pure Re and pure W. They are very close to the experimental data of Ref. 25, and relaxation lowers the energy by just 8 and 4 meV/atom for Re and W, respectively. This energy difference is very small not only for the pure elements, but for all configurations considered in this study, as can be seen by comparing Figs. 2 and 3. As these energy differences are much smaller than the smallest difference between the formation energies of any of the 42 configurations, it follows that relaxation effects are, surprisingly, without consequence for the study of the thermodynamically stable configurations of the Re-W sigma based system.

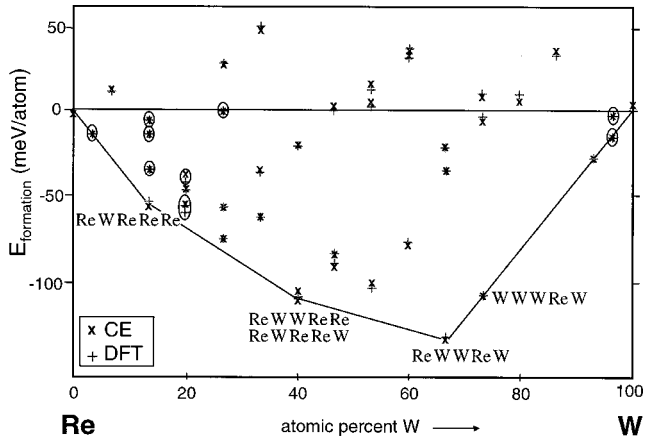

FIG. 3. Formation energy (in meV/atom) of relaxed atomic configurations with the sigma structure: as computed with VASP (+); as computed from the effective interactions (×). Circles indicate the sigma superstructures. The most stable configurations have been connected with a solid line and the occupancy of the *A*, *B*, *C*, *D*, and *E* sites have been indicated.

TABLE IV. Values of the 29 effective cluster interactions (units are in K) for Re-W system; degeneracy is given in parentheses.

Sites	A (2)	B (4)	C (8)	D (8)	E (8)	
Site energies	111	−491	−736	100	−900	
Pairs (distance)	AD (8) (2,94 Å)	AE (8) (3,14 Å)	AB (8) (3,26 Å)	DD (4) (3,01 Å)	DC (8) (3,06 Å)	DC (8) (3,07 Å)
Pair interactions	70	95	51	128	194	135
Pairs (distance)	DC (16) (3,10 Å)	DE (16) (3,15 Å)	DE (16) (3,18 Å)	BC (8) (3,02 Å)	BB (2) (3,19 Å)	BD (16) (3,35 Å)
Pair interactions	342	499	−138	210	−53	79
Pairs (distance)	CC (4) (2,89 Å)	CE (16) (3,45 Å)	CE (16) (3,50 Å)	CC (16) (3,54 Å)	EE (4) (2,84 Å)	DE (8) (3,53 Å)
Pair interactions	71	332	−45	−65	353	−14
Triangles and tetrahedron	ABD (16)	BDE (16)	BDC (16)	DEC (16)	AEBD (16)	
Multiplets interactions	39	50	−106	−194	−74	

Figures 2 and 3 give indications about the convergence of the CWM method as well. As explained in Sec. III, a singular value decomposition algorithm was used to ''fit'' the values for 29 effective interactions from the formation energies of the 42 configurations. The effective interactions reproduce the formation energies very well, as is illustrated in Figs. 2 and 3. The effective interactions can be used to calculate the formation energies of configurations not used in the ''fit'' and compared with first-principles results. The difference is a measure of the ''predictive error'' [20] in this case less than 4 meV/atom. The interactions are given in Table IV. For multisite terms, we have used *A, B, C, D*, and *E* site labels to indicate what kind of sites are connected.

B. Site occupancy

The interactions were used to compute the site occupancy via the calculation of the Gibbs free energy as a function of temperature and composition within the tetrahedron approximation of the cluster variation method. Figures 4 and 5 show the site preference for temperatures of 500 and 1500 K. In both figures the site occupancy sequence as a function of W composition is the same, although it is less pronounced at 1500 K. First the *B* site is filled with W, next the sites *C* and *E* are filled, and last the *A* and *D* sites are filled. Once the *B* site has been filled with W and the W content ranges from 20 to 70%, a site competition occurs between the 14-fold coordinated *C* and *E* sites (see Fig. 4). When the W content is increased further from 70 to 100%, the two icosahedral *A* and *D* sites.

Comparing the results calculated at 500, 1000, 1500, and 2000 K with the neutron-diffraction data an excellent agreement is found, especially concerning the occupancy sequence of the five sites (see Table V). It seems that the theoretical results obtained at high temperatures are quantitatively in better agreement with the experimental data. This is not surprising considering that the samples have

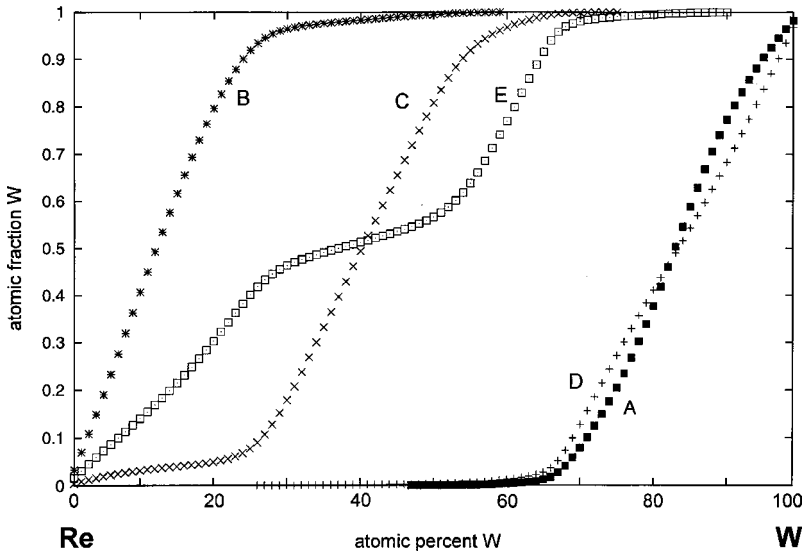

FIG. 4. Computed occupancy of the inequivalent sites in the sigma phase at 500 K.

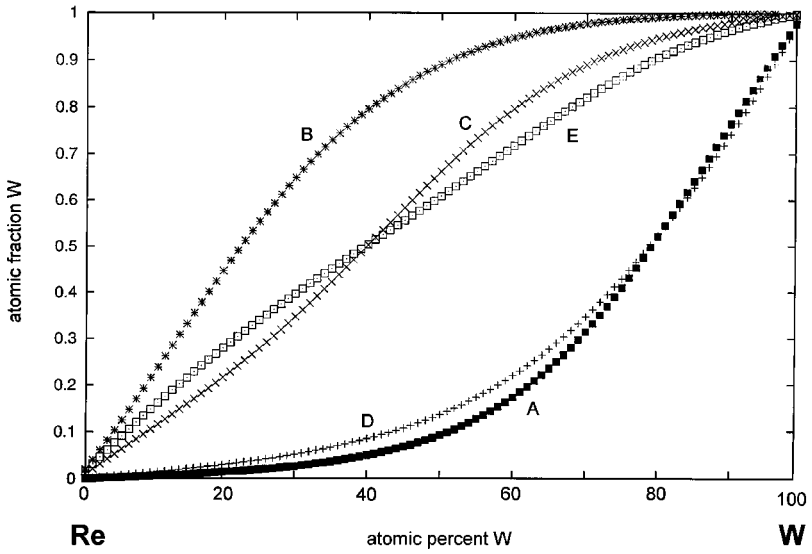

FIG. 5. Computed occupancy of the inequivalent sites in the sigma phase at 1500 K.

been prepared with a solidification process characterized by moderate cooling rates. The cooling rate does not modify the main conclusions regarding the site occupancy as will be discussed in a forthcoming paper.

The occupancy sequence can be understood from the single-site and multisite interactions listed in Table IV. Negative single-site interactions indicate W preference. Table IV shows that *E* and *C* sites have a strong W preference, followed by the *B* site, while the *A* and *D* sites have Re preference. Previous results obtained for pure transition metals in different FK structures[26] explain the clear preference for W to occupy the *B*, *C*, and *E* sites and for Re to occupy the *A* and *D* sites. It was shown that the band energy is reduced most when a transition metal with the larger number of states near the Fermi level occupies the low-symmetry sites, while a transition metal with the smaller number is positioned at the high-symmetry sites. This usually means that transition metals with half *d*-band filling predominantly occupy the highly coordinated *B*, *C*, and *E* sites while transition metals with nearly filled or nearly empty *d* bands occupy the icosahedral *A* and *D* sites.

However, neither this argument nor the single-site interactions are insufficient to explain the competition between the *B*, *C*, and *E* sites. In fact the *B*-*C*-*E* sequence results from a subtle competition between single-site and multisite interactions. Table IV shows that the pair interactions between two *B* sites favors W occupancy while *E*-*E* pairs occupied by W are disfavored (a negative sign of a pair interaction means a favorable W-W pair). The *CC* pairs are of mixed attractive and repulsive type. Thus both single-site and pair interactions contribute to the filling of the *B* site by

TABLE V. Calculated site occupancy at four different temperatures. Comparison with experimental data.

	Site	500 K	1000 K	1500 K	2000 K	Experimental
σ-WRe 34% W	*A*	0% W	0–1% W	2,5% W	5% W	5% W±3%
	B	97% W	83% W	73% W	65% W	60% W±2%
	C	30% W	40% W	42% W	42% W	46% W±2%
	D	0% W	0–1% W	5% W	10% W	2% W±4%
	E	48% W	43% W	42% W	42% W	47% W±2%
σ-WRe 44% W	*A*	0% W	1% W	6% W	10% W	7% W±3%
	B	99% W	93% W	86% W	78% W	72% W±2%
	C	68% W	58% W	58% W	57% W	62% W±3%
	D	0% W	2% W	8% W	13% W	8% W±3%
	E	52% W	53% W	56% W	54% W	56% W±2%
σ-WRe 54% W	*A*	0% W	5% W	10% W	17% W	16% W±3%
	B	100% W	98% W	92% W	87% W	92% W±2%
	C	90% W	78% W	73% W	68% W	75% W±1%
	D	0% W	5% W	14% W	22% W	6% W±2%
	E	67% W	67% W	67% W	63% W	70% W±1%

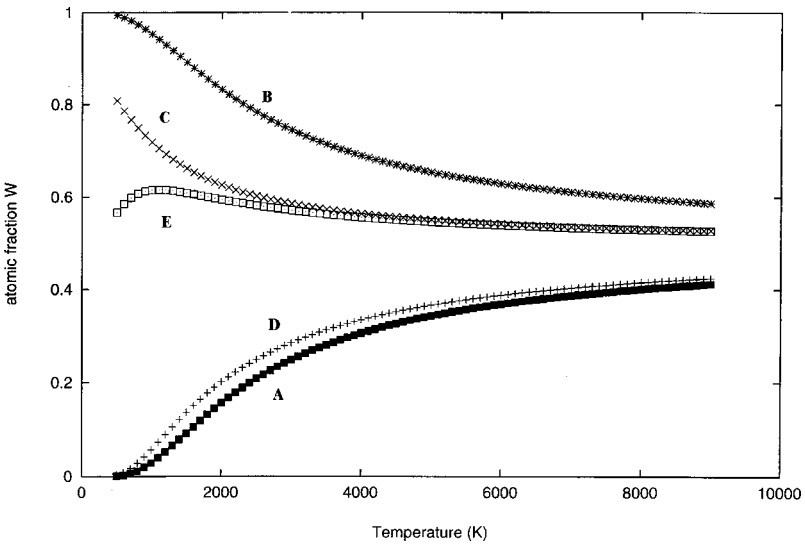

FIG. 6. Computed occupancy of the inequivalent sites in the $Re_{0.5}W_{0.5}$ sigma phase as a function of temperature.

W atoms while single-site and pair interactions counteract each other in the filling of the *E* sites by W atoms.

In the same way the competition between the *C* and *E* sites at low temperatures can be explained from the interplay of single-site and multisite interactions. The single-site interaction favors W occupancy of the *E* site but when the *E* site is gradually filled, the pairwise disadvantage for the *E* sites appears because W atoms on neighboring *E* sites strongly repel each other. W atoms on neighboring *C* sites weakly attract or weakly repel each other, so that at higher W occupancy, the *C* site becomes favorable over the *E* site. This frustrated site occupation behavior that has been predicted for the Fe-Cr sigma alloys as well,[10] can be vaguely recognized in the experimental data. Table I indicates that for a sigma phase with 34% W, the *C* and *E* sites have 46 and 47% W, respectively, while for a sigma phase with 54% W, the *C* and *E* sites have 75 and 70% W, respectively. However, in this range of composition, the differences remain too small to firmly establish this reversal of site occupancy between *C* and *E* sites. The *B, E* and *C, D*, and *A* site occupation sequence found in the Re-W is not the same as the *E, C, B, A*, and *D* sequence in the Fe-Cr system. While the division of *AD* and *BCE* sites is the same, the sequences within the two groups can be explained only by subtle alloying effects which depend on the specific system.

In Fig. 6, the site occupancy of a $Re_{0.5}W_{0.5}$ alloy is shown as a function of the temperature. At high temperatures, the site occupancy very slowly reaches the value corresponding to the random configuration. This limit occupancy being determined purely by the alloy composition, in this case, the limit of each site is 50% W. However, as already discussed previously,[10] this limit is reached asymptotically because no order-disorder transformation takes place in the system. In the equiatomic alloy, the *C* and *E* sites have the most mixed occupancy. When the temperature is lowered, the fraction of W increases a little on the *C* site and increases a lot on the *B* site, concurrently the fraction of Re increases on the *A* and *D* sites. The *E* site displays a curious behavior in contrast to the other four sites. Descending from a high temperature, the site exhibits a W-type preferential occupancy but around 1000 K, the W occupancy is lowered until at very low temperature a certain limit value is reached. This apparent reversal of the

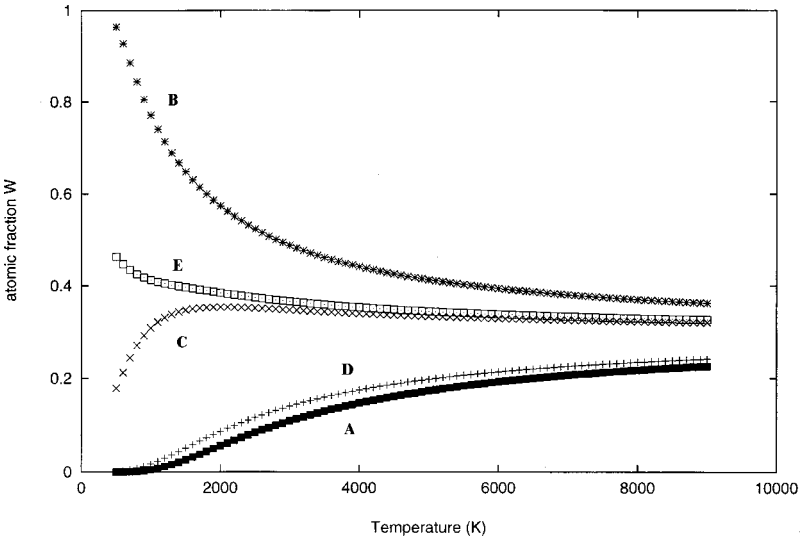

FIG. 7. Computed occupancy of the inequivalent sites in the $Re_{0.7}W_{0.3}$ sigma phase as a function of temperature.

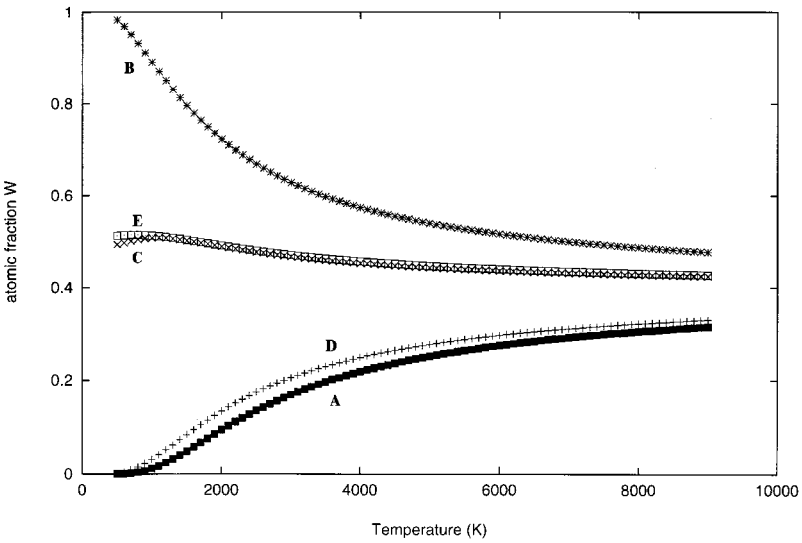

FIG. 8. Computed occupancy of the inequivalent sites in the $Re_{0.6}W_{0.4}$ sigma phase as a function of temperature.

site occupation arises again from the competition between *E* and *C* site occupancy via the single-site and multisite interactions. CVM calculations show that it occurs over a wide range of compositions but depends on the alloy composition (see Figs. 7 and 8). For a sigma phase with 50% W, the *E* site is frustrated while for a sigma phase with 30% W, it is the *C* site which is frustrated leading to two distinct temperature-dependent reversal phenomena. For a sigma phase with 40% W, both *E* and *C* sites display site preference reversal behavior as a function of temperature.

V. CONCLUSION

The site occupancy in the Re-W sigma phase has been investigated using both experimental and theoretical approaches. It is shown that the five crystallographically inequivalent sites produce a number of peculiarities. With increasing W composition, both experimental and theoretical investigations indicate that first the *B* site is filled followed by the *C* and *E* sites and next by the *A* and *D* sites.

The site preference in Re-W and Fe-Cr sigma phases follows the same general classification that is based on arguments from studies of the relative stability of FK phases in pure metals. In short, the icosahedral *A* and *D* sites prefer Fe and Re which have a smaller number of states near the Fermi level, while the higher coordinated and less symmetric *B*, *C*, and *E* sites prefer Cr and W which have a greater number of states near the Fermi level. The Re-W result differs from that obtained in the Fe-Cr sigma phase in the site preference sequence for the less symmetric sites. The subtle competition on the *B*, *C*, and *E* sites cannot be understood from a simple examination of the atom species alone. In the context of the Ising-type Hamiltonian, the site occupation sequence results from a competition between single-site and multisite interactions.

[1] D. de Fontaine, Solid State Phys. **34**, 73 (1979).
[2] F. Ducastelle, *Order and Phase Stability in Alloys*, *Cohesion and Structure*, edited by F. R. de Boer and D. G. Pettifor (North-Holland, Amsterdam, 1991), Vol. 3.
[3] A. K. Sinha, Prog. Mater. Sci. **15**, 79 (1973).
[4] R. E. Watson and L. H. Bennett, Acta Metall. **32**, 477 (1984).
[5] P. E. A. Turchi, G. Treglia, and F. Ducastelle, J. Phys. F: Met. Phys. **13**, 2543 (1983).
[6] R. Phillips and A. E. Carlsson, Phys. Rev. B **42**, 3345 (1990).
[7] P. E. A. Turchi and A. Finel, Phys. Rev. B **46**, 702 (1992).
[8] F. Ducastelle and F. Gautier, J. Phys. F: Met. Phys. **6**, 2039 (1976).
[9] R. Kikuchi, Phys. Rev. **81**, 998 (1951); J. M. Sanchez, F. Ducastelle, and D. Gratias, Physica A **128**, 334 (1984).
[10] M. Sluiter, K. Esfarjani, and Y. Kawazoe, Phys. Rev. Lett. **75**, 3142 (1995).
[11] H. L. Yakel, Acta Crystallogr., Sect. B: Struct. Sci. **B39**, 20 (1983).
[12] S. M. Dubiel and B. F. O. Costa, Phys. Rev. B **47**, 12 257 (1993).
[13] J. L. C. Daams, P. Villars, and J. H. N. van Vucht, *Atlas of Crystal Structures for Intermetallic Phases* (ASM International, Materials Park, OH, 1991), p. 3804.
[14] H. M. Rietveld, J. Appl. Crystallogr. **2**, 65 (1969).
[15] J. Rodriguez-Carjaval, Physica B **192**, 55 (1993).
[16] G. Cagliotti, A. Paoletti, and F. P. Ricci, Nucl. Instrum. **3**, 223 (1958).
[17] D. de Fontaine, in *Alloy Phase Stability*, edited by G. M. Stocks and A. Gonis (Kluwer Academic, Boston, 1989), p. 177.
[18] J. W. D. Connolly and A. R. Williams, Phys. Rev. B **27**, 5169 (1983).
[19] M. Sluiter, D. de Fontaine, X. Q. Guo, R. Podloucky, and A. J. Freeman, Phys. Rev. B **42**, 10 460 (1990).
[20] M. Sluiter, Y. Watanabe, D. de Fontaine, and Y. Kawazoe, Phys. Rev. B **53**, 6137 (1996).
[21] G. Kresse and G. Furthmueller, Phys. Rev. B **54**, 11 169 (1996).
[22] G. Kresse and J. Hafner, J. Phys.: Condens. Matter **6**, 8245 (1994).

[23] M. Methfessel and A. T. Paxton, Phys. Rev. B **40**, 3616 (1989).
[24] A. Pasture and B. Vinet, in *Phase Transformations and Systems Driven Far from Equilibrium*, edited by E. En Ma, P. Bellon, M. Atzmon, and R. Trivedi, Mater. Res. Soc. Symp. Proc. No. 481, (Materials Research Society, Pittsburgh, 1998), p. 27.
[25] C. G. Wilson, Acta Crystallogr. **16**, 724 (1963).
[26] C. Berne, A. Pasturel, M. Sluiter, and B. Vinet, Phys. Rev. Lett. **83**, 1621 (1999).